Inorg. Chem. **2002**, *41*, 3302–3307

Hydrothermal Synthesis, Structures, and Magnetic Properties of Three Novel 5-Aminoisophthalic Acid Ligand Bridged Transition Metal Cation Polymers

Chuan-De Wu, Can-Zhong Lu,* Wen-Bin Yang, Hong-Hui Zhuang, and Jin-Shun Huang

The State Key Laboratory of Structural Chemistry, Fujian Institute of Research on the Structure of Matter, The Chinese Academy of Sciences, Fuzhou, Fujian, 350002, P.R. China

Received November 16, 2001

Three novel 5-aminoisophthalic acid (AIP) bridged polymers $[Co(C_8NH_5O_4)(H_2O)]_n$ (**1**), $[Ni(C_8NH_5O_4)(H_2O)_2]_n$ (**2**), and $[Zn(C_8NH_5O_4)(H_2O)]_n$ (**3**) were synthesized by hydrothermal reactions and characterized by IR, Raman, elemental analysis, ESR, and magnetic measurements. X-ray single-crystal analyses were carried out for $[Co(C_8NH_5O_4)(H_2O)]_n$ (**1**), which crystallizes in the triclinic system, space group $P\bar{1}$, with $a = 6.477(1)$ Å, $b = 7.130(1)$ Å, $c = 9.826(2)$ Å, $\alpha = 108.9(1)°$, $\beta = 93.97(3)°$, $\gamma = 98.82(3)°$, and $Z = 2$; for $[Ni(C_8NH_5O_4)(H_2O)_2]_n$ (**2**), in the triclinic system, space group $P\bar{1}$, $a = 6.425(1)$ Å, $b = 8.115(2)$ Å, $c = 10.146(2)$ Å, $\alpha = 113.09(3)°$, $\beta = 99.64(3)°$, $\gamma = 98.90(3)°$, and $Z = 2$; and for $[Zn(C_8NH_5O_4)(H_2O)]_n$ (**3**), in the monoclinic system, space group $P2(1)/n$, $a = 9.044(1)$ Å, $b = 8.264(1)$ Å, $c = 11.646(1)$ Å, $\beta = 100.77(1)°$, and $Z = 4$. The single X-ray diffraction studies reveal that **1** consists of an infinite honeycomb layer formed by four crystallographically independent motifs packed alternatively together; **2** consists of an infinite neutral railroad-like linear polymer, and **3** consists of infinite layers of alternating four-coordinated Zn(II) cations and AIP ligands. Finally, they are all packed into beautiful three-dimensional frameworks through complicated hydrogen bonding. Antiferromagnetic and ferromagnetic behaviors were observed for **1** and **2** from the magnetic measurements.

1. Introduction

Owing to the enormous variety of intriguing structural topologies and their unexpected properties for potential practical applications,[1−21] the chemistry of novel metal−organic coordination polymers based on covalent interaction[22,23] or supramolecular contacts (such as hydrogen bonding and/or $\pi-\pi$ stacking interactions)[24−32] has been

* To whom correspondence should be addressed. E-mail: czlu@ms.fjirsm.ac.cn.

(1) Blake, A. J.; Champness, N. K.; Hubbersley, P.; Li, W.-S.; Withersly, M. A.; Schöder, M. *Coord. Chem. Rev.* **1999**, *183*, 117.
(2) Yaghi, O. M.; Li, H.; Davis, C.; Richardson, D.; Groy, T. L. *Acc. Chem. Res.* **1998**, *31*, 474.
(3) Hagrman, P. J.; Hagrman, D.; Zubieta, J. *Angew. Chem., Int. Ed.* **1999**, *38*, 2638.
(4) Batten, S. R. Robson, R. *Angew. Chem., Int. Ed.* **1998**, *37*, 1460.
(5) Stupp, S. I.; Braun, P. V. *Science* **1997**, *277*, 1242.
(6) Zaworotko, M. J. *Chem. Soc. Rev.* **1994**, 283.
(7) Hamers, C.; Kocian, O.; Raymo, F. M.; Stoddard, J. F. *Adv. Mater.* **1998**, *10*, 1366 and references therein.
(8) Mitzi, D. B.; Wang, S.; Field, C. A.; Chess, C. A.; Guloy, A. M. *Science* **1995**, *267*, 1473.
(9) Wang, S.; Mitzi, D. B.; Field, C. A.; Guloy, A. *J. Am. Chem. Soc.* **1995**, *117*, 5297.
(10) Matsumoto, N.; Sunatsuki, Y.; Miyasaka, H.; Hashimoto, Y.; Luneau, D.; Tuchagues, J.-P. *Angew. Chem., Int. Ed.* **1999**, *38*, 171.
(11) Triki, S.; Pala, J. S.; Decoster, M.; Molinié, P.; Toupet, L. *Angew. Chem., Int. Ed.* **1999**, *38*, 113.
(12) Miller, J. S.; Epstain, A. J. *Chem. Commun.* **1998**, 1319.
(13) Buschmann, A. W. E.; Arit, M.; Miller, J. S. *Angew. Chem., Int. Ed.* **1998**, *37*, 781.
(14) Li, H.; Eddaoudi, M. O.; Yaghi, O. M. *Nature* **1999**, *402*, 276.
(15) Yaghi, O. M.; Li, H. *J. Am. Chem. Soc.* **1996**, *118*, 295.
(16) Venkataraman, D.; Gardner, G. B.; Lee, S.; Moore, J. S. *J. Am. Chem. Soc.* **1995**, *117*, 11600.
(17) Carlucci, L.; Ciani, G.; Proserpio, D. M.; Soroni, A. *J. Am. Chem. Soc.* **1995**, *117*, 4562.
(18) Chui, S. S.-Y.; Lo, S. M.-F.; Charmant, S. P. H.; Orpen, A. G.; Williams, L. D. *Science* **1999**, *283*, 1148 and references therein.
(19) Yamamoto, H. M.; Yamaura, J.; Kato, R. *J. Am. Chem. Soc.* **1998**, *120*, 5905.
(20) Li, H.; Eddaoudi, M.; Groy, T. L.; Yaghi, O. M. *J. Am. Chem. Soc.* **1998**, *120*, 8571.
(21) Janiak, C. *Angew. Chem., Int. Ed. Engl.* **1997**, *36*, 1431.
(22) Robson, R.; Abrahams, B. F.; batten, S. R.; Grable, R. W.; Hoskins, B. F.; Liu, J. *Supramolecular Architecture*; American Chemical Society: Washington, DC, 1992; Chapter 19.
(23) Fujita, M.; Kwon, Y. J.; Washizu, S.; Ogura, K. *J. Am. Chem. Soc.* **1994**, *116*, 1151.
(24) Desiraju, G. R. *Crystal Engineering: The Design of Organic Solids*; Elsevier: Amsterdam, 1989.
(25) Desiraju, G. R. *Angew. Chem., Int. Ed. Engl.* **1995**, *35*, 2311.
(26) Janiak, C. *J. Chem. Soc., Dalton Trans.* **2000**, 3885 and references therein.

10.1021/ic011182g CCC: $22.00
Published on Web 05/18/2002

actively investigated. The vast majority of reported work is based upon the use of polyfunctional organic ligands to bind to the d-block transition metal ions through self-assembly processes, leading to the formation of compounds with fascinating topologies and physical properties. It has also been proved that the careful selection of appropriate multidentate bridging ligands is helpful not only to tailor effectively the polymer architectures but also to realize various applications. In the hydrothermal synthesis field, studies have been focused on organic−inorganic hybrid materials containing N-donor rigid heteroaroarmatic ligands, such as pyrazine or 4,4′-bipyridine. However, much less work has been carried out to investigate transition metal polymer aminobenzoic acid ligands. The structures of N-donor analogues are expected to be more difficult to control due to the more flexible coordination manner of the amino group. In the course of our investigation on the synthesis of transition metal materials, we have synthesized some unprecedented structures by using some aminobenzoic acids, such as 5-aminoisophthalic acid (AIP)[33] as a bridging ligand, which has two carboxylate groups and particularly one amino group. Here, we report the preparations and X-ray structures of three novel AIP-bridged polymers, $[Co(C_8NH_5O_4)(H_2O)]_n$ (**1**), $[Ni(C_8NH_5O_4)(H_2O)_2]_n$ (**2**), and $[Zn(C_8NH_5O_4)(H_2O)]_n$ (**3**), with very different architectures. The magnetic properties of **1** and **2** have also been studied.

2. Experimental Section

2.1. Materials and Methods. All chemicals were of reagent grade and were used as received. Elemental analyses were performed with a Vario EL III CHNOS element analyzer. Infrared spectra were recorded on a FTS-40 spectrophotometer using pressed KBr pellets. The FT-Raman spectra were measured on a Nicolet Raman 910 Fourier transform laser-Raman spectrum, again using pressed KBr pellets, and ESR spectra were performed on a Bruker ER 420 instrument. Variable-temperature magnetic susceptibilities in the temperature range 5−300 K were measured on a model CF-1 superconducting extracting sample magnetometer with the powdered sample kept in the capsule for weighing. All data were corrected for diamagnetism of the ligands estimated from Pascal's constants.[34]

2.2. Synthesis. All syntheses were performed in sealed 30 mL Teflon-lined stainless steel vessels.

$[Co(C_8NH_5O_4)(H_2O)]_n$ (1). A mixture of $CoSO_4 \cdot 7H_2O$ (0.19 g, 0.68 mmol) and 5-aminoisophthalic acid (0.12 g, 0.66 mmol) in H_2O (18 mL) was heated at 170 °C for 6 days under autogenous pressure. After the reaction was slowly cooled to room temperature, deep red crystals were produced (yield: 69%, based on Co). Anal. Calcd for $C_8H_7CoNO_5$ (%): C, 37.52; H, 2.76; N, 5.47. Found (%): C, 37.85; H, 2.92; N, 5.53. IR (solid KBr pellet ν/cm^{-1}): 1684s, 1620m, 1545s, 1481m, 1437m, 1398s, 1331m, 1298s, 1271m, 1242s, 1138w, 1103sh, 1078m, 1047m, 1001m, 957s, 802w, 766s, 727w, 690m, 669m, 592m, 567sh, 444m. FT-Raman (solid, λ = 1064 nm, ν/cm^{-1}): 1683s, 1606s, 1554w, 1442sh, 1401s, 1299m, 1182w, 1077m, 100vs, 798m, 771w, 688w, 651w, 472m, 449m, 385m, 206s, 189s, 169m.

$[Ni(C_8NH_5O_4)(H_2O)_2]_n$ (2). A mixture of $NiCl_2 \cdot 6H_2O$ (0.10 g, 0.42 mmol) and 5-aminoisophthalic acid (0.08 g, 0.44 mmol) in H_2O (18 mL) was heated at 170 °C for 6 days under autogenous pressure. Deep green crystals were isolated after the reaction solution was cooled gradually and then washed with water and ethanol (yields: 66.2%, based on Ni). Anal. Calcd for $C_8H_9NNiO_6$ (%): C, 39.12; H, 4.10; N, 5.70. Found (%): C, 39.05; H, 4.06; N, 5.63. IR (solid KBr pellet ν/cm^{-1}): 1618s, 1531s, 1487s, 1446m, 1429m, 1379s, 1329m, 1271m, 1144m, 1105s, 999m, 974s, 935s, 895m, 818m, 806m, 781s, 727s, 687s, 625m, 592m, 461m, 422m. FT-Raman (solid, λ = 1064 nm, ν/cm^{-1}): 1947m, 1847m, 1617s, 1569m, 1482m, 1448s, 1419s, 1369m, 1276m, 1097m, 998s, 967m, 804s, 603m, 563m, 476m, 458m, 433m, 420m, 385m, 254m, 229m, 159s, 132m.

$[Zn(C_8NH_5O_4)(H_2O)]_n$ (3). The pH of a mixture of $Zn(OCOCH_3)_2 \cdot 2H_2O$ (0.15 g, 0.68 mmol) and 5-aminoisophthalic acid (0.12 g, 0.66 mmol) in H_2O (18 mL) was adjusted to 3.90 with vigorous stirring, and then the resultant mixture was heated at 170 °C for 6 days. Light brown crystals were isolated after the reaction solution was cooled gradually and then washed with water and ethanol (yields: about 56.8%, based on Zn). Anal. Calcd for $C_8H_7NO_5Zn$ (%): C, 36.60; N, 5.34; H, 2.69. Found (%): C, 36.19; N, 5.43; H, 2.86. IR (solid KBr pellet ν/cm^{-1}): 1624s, 1576m, 1552s, 1483m, 1441m, 1410s, 1363s, 1325sh, 1157s, 1126m, 1117m, 1003m, 968m, 937m, 901m, 843m, 802m, 773s, 741s, 677m, 650m, 600m, 575m, 538s, 463m, 420m. FT-Raman (solid, λ = 1064 nm, ν/cm^{-1}): 1625m, 1602s, 1560m, 1440m, 1409vs, 1355m, 1263m, 1168s, 1124m, 1002vs, 962m, 805m, 537w, 412m, 356m, 240s, 213m, 138s, 123m.

2.3. Crystal Structure Determination. The determination of the unit cells and the data collections for a deep red crystal of compound **1** and a deep green crystal of compound **2** were performed on an Enraf-Nonius CAD4 diffractometer with graphite-monochromatized Mo Kα radiation (λ = 0.71073 Å) at 293 K. Lorentz−polarization corrections and an empirical absorption were applied to the data. The determination of the unit cell and the data collection for a light brown crystal of compound **3** were performed on a Siemens SMART CCD, and the data were collected using graphite-monochromatized Mo Kα radiation (λ = 0.71073 Å) at 293 K. The data set was corrected by the SADABS program.[35] The structures of **1** and **3** were both solved by direct methods, while the structure of **2** was solved by the Patterson method and all of the structures were refined by a full-matrix least-squares method with the SHELXL-97[36] program package. All atoms except hydrogen atoms were refined anisotropically. Crystallographic data are summarized in Table 1, and selected bond lengths and angles are listed in Table 2, while selected hydrogen bond distances (Å) and angles (deg) are listed in Table 3, respectively.

3. Results and Discussion

3.1. Syntheses and Structures. The syntheses of compounds **1** and **2** reported here were simply synthesized by

(27) Blake, A. J.; Champness, N. R.; Cooke, P. A.; Nicolson, J. E. B.; Wilson, C. *J. Chem. Soc., Dalton Trans.* **2000**, 3811.
(28) Nakash, M.; Clyde-Watson, Z.; Feeder, N.; Teat, S. J.; Sanders, J. K. M. *Chem. Eur. J.* **2000**, *6*, 2112.
(29) Burrows, A. D.; Harrington, R. W.; Mahon, M. F.; Price, C. E. *J. Chem. Soc., Dalton Trans.* **2000**, 3845.
(30) Plater, J. M.; Foreman, M. R. St. J.; Gelbrich, T.; Coles, S. J.; Hursthouse, M. B. *J. Chem. Soc., Dalton Trans.* **2000**, 3065.
(31) Janiak, C.; Deblon, S.; Wu, H.-P.; Kolm, M. J.; Klufers, P.; Piotrowski, H.; Mayer, P. *Eur. J. Inorg. Chem.* **1999**, 1507.
(32) Janiak, C.; Temizdemir, S.; Scharmann, T. G.; Schmalstieg, A.; Demtschuk, J. *Z. Anorg. Allg. Chem.* **2000**, *626*, 2053.
(33) Dobson, A. J.; Gerkin, R. E. *Acta Crystallogr.* **1998**, *C54*, 1503.
(34) Pascal, P. *Ann. Chim. Phys.* **1910**, *19*, 5.
(35) Sheldrick, G. M. *SADABS*; Siemens Analytical X-ray Instrument Division: Madison, WI, 1995.
(36) Sheldrick, G. M. Universität Göttingen, Germany, 1997.

Table 1. Crystal Data and Structure Refinement for $[Co(C_8NH_5O_4)(H_2O)]_n$ (**1**), $[Ni(C_8NH_5O_4)(H_2O)_2]_n$ (**2**), and $[Zn(C_8NH_5O_4)(H_2O)]_n$ (**3**)

	1	**2**	**3**
formula	$C_8H_7CoNO_5$	$C_8H_9NNiO_6$	$C_8H_7NO_5Zn$
fw	256.08	307.74	262.52
cryst syst	triclinic	triclinic	monoclinic
space group	$P\bar{1}$	$P\bar{1}$	$P2(1)/n$
a (Å)	6.477(1)	6.425(1)	9.044(1)
b (Å)	7.130(1)	8.115(2)	8.264(1)
c (Å)	9.826(2)	10.146(2)	11.646(1)
α (deg)	108.9(1)	113.09(3)	90
β (deg)	93.97(3)	99.64(3)	100.77(1)
γ (deg)	98.82(3)	98.90(3)	90
V (Å^3)	420.8(2)	465.4(2)	855.0(2)
Z	2	2	4
D_{calcd} (g cm^{-3})	2.021	1.955	2.039
μ (Mo Kα) (mm^{-1})	2.038	2.098	2.872
λ (Å)	0.71073	0.71073	0.71073
T (°C)	20	20	20
R1, wR2 [$I > 2\sigma(I)$][a]	0.0283, 0.0743	0.0699, 0.1756	0.0422, 0.1047
R1, wR2 (all data)	0.0306, 0.0752	0.0901, 0.1826	0.0568, 0.1148

[a] $R1 = \sum(|F_o| - |F_c|)/\sum|F_o|$. $wR2 = [\sum w(F_o^2 - F_c^2)^2/\sum w(F_o^2)^2]^{1/2}$.

mixing Co(II) or Ni(II) with the AIP ligand in almost equal molar ratio under hydrothermal reaction conditions. Interestingly, no product could be obtained from the reaction of zinc(II) acetate and the AIP ligand under similar hydrothermal reaction conditions, which might result from the following reasons: (1) The presence of the AIP ligand in the reaction mixture is not only to act as a necessary coordination ligand but also to influence the pH value of the reaction mixture. (2) When Co(II) or Ni(II) was mixed with the AIP ligand in almost equal molar ratio, the pH was equal to 3.76 or 3.49, which might be helpful for the formation of polymers **1** and **2**. However, when zinc(II) acetate and AIP ligand were mixed together, the pH was 4.76, which might not be the best value for the formation of **3**. Thus, when the pH was adjusted to the 1.34−3.90 range, compound **3** was obtained as light brown blocks under similar hydrothermal reaction conditions.

Single-crystal X-ray diffraction study reveals that polymer **1**, which crystallizes in the space group $P\bar{1}$, consists of an infinite honeycomb layer formed by four crystallographically independent motifs packed alternatively together. The ORTEP representation of the symmetry for the expanded local structure of **1** is illustrated in Figure 1, and a view of the

Table 2. Selected Bond Lengths (Å) and Angles (deg) for **1**, **2**, and **3**[a]

		Complex **1**			
Co(1)−O(5)^{i}	2.012(2)	O(5)#1−Co(1)−O(1)^{ii}	158.1(1)	O(5)^{i}−Co(1)−O(3)^{ii}	98.0(1)
Co(1)−O(1)^{ii}	2.098(2)	O(5)#1−Co(1)−O(2)^{iii}	96.2(1)	O(1)^{ii}−Co(1)−O(3)^{ii}	60.9(1)
Co(1)−O(2)^{iii}	2.114(2)	O(1)#2−Co(1)−O(2)^{iii}	91.0(1)	O(2)^{iii}−Co(1)−O(3)^{ii}	92.8(1)
Co(1)−O(4)	2.147(2)	O(5)#1−Co(1)−O(4)	92.0(1)	O(4)−Co(1)−O(3)^{ii}	169.4(1)
Co(1)−N(1)	2.186(2)	O(1)#2−Co(1)−O(4)	108.8(1)	N(1)−Co(1)−O(3)^{ii}	93.3(1)
Co(1)−O(3)^{ii}	2.211(2)	O(2)#3−Co(1)−O(4)	89.8(1)	C(1)−O(1)−Co(1)^{ii}	91.9(1)
O(1)−C(1)	1.271(3)	O(5)#1−Co(1)−N(1)	87.8(1)	C(8)−O(2)−Co(1)^{iv}	121.5(2)
O(2)−C(8)	1.274(3)	O(1)#2−Co(1)−N(1)	87.6(1)	C(1)−O(3)−Co(1)^{ii}	87.3(1)
O(3)−C(1)	1.253(3)	O(2)#3−Co(1)−N(1)	172.2(1)	C(8)−O(5)−Co(1)^{i}	131.3(2)
O(5)−C(8)	1.256(3)	O(4)−Co(1)−N(1)	83.4(1)	C(4)−N(1)−Co(1)	118.2(2)
		Complex **2**			
Ni−O(4)^{v}	2.030(3)	O(4)^{v}−Ni−O(5)	89.1(1)	O(4)^{v}−Ni−O(2)	100.4(1)
Ni−O(5)	2.046(3)	O(4)^{v}−Ni−O(6)	96.0(1)	O(5)−Ni−O(2)	90.2(1)
Ni−O(6)	2.052(4)	O(5)−Ni−O(6)	91.5(2)	O(6)−Ni−O(2)	163.5(1)
Ni−O(1)	2.091(3)	O(4)^{v}−Ni−O(1)	162.3(1)	O(1)−Ni−O(2)	61.9(1)
Ni−N(1)^{vi}	2.117(4)	O(5)−Ni−O(1)	92.2(2)	N(1)^{vi}−Ni−O(2)	93.8(1)
Ni−O(2)	2.156(3)	O(6)−Ni−O(1)	101.6(1)	C(1)−O(1)−Ni	90.2(2)
O(1)−C(1)	1.259(5)	O(4)^{v}−Ni−N(1)^{vi}	89.5(1)	C(1)−O(2)−Ni	87.3(3)
O(2)−C(1)	1.256(5)	O(5)−Ni−N(1)^{vi}	176.0(2)	C(5)−O(4)−Ni^{vii}	129.8(3)
O(3)−C(5)	1.245(6)	O(6)−Ni−N(1)^{vi}	84.9(2)	C(7)−N(1)−Ni^{vi}	119.4(3)
O(4)−C(5)	1.272(5)	O(1)−Ni−N(1)^{vi}	90.3(1)		
		Complex **3**			
Zn(1)−O(2)^{viii}	1.954(3)	O(2)^{viii}−Zn(1)−O(3)	109.4(2)	O(2)^{viii}−Zn(1)−N(1)	105.1(2)
Zn(1)−O(3)	1.965(4)	O(2)^{viii}−Zn(1)−O(5)^{ix}	94.9(1)	O(3)−Zn(1)−N(1)	118.0(2)
Zn(1)−O(5)^{ix}	1.973(3)	O(3)−Zn(1)−O(5)^{ix}	10.4(2)	O(5)^{ix}−Zn(1)−N(1)	116.1(2)
Zn(1)−N(1)	2.031(4)				

[a] Symmetry transformations used to generate equivalent atoms: (i) $-x+1, -y+1, -z+2$; (ii) $-x+1, -y, -z+1$; (iii) $x-1, y-1, z$; (iv) $x+1, y+1, z$; (v) $x, y, z+1$; (vi) $-x+1, -y+2, -z+2$; (vii) $x, y, z-1$; (viii) $x-{}^1/_2, -y+{}^1/_2, z+{}^1/_2$; (ix) $x, y-1, z$.

Table 3. Selected Hydrogen Bonds Lengths (Å) for **1**, **2**, and **3**[a]

1			**2**			**3**		
D−H	d(D···A)	A	D−H	d(D···A)	A	D−H	d(D···A)	A
O4−H2	2.833	O2^{i}	O5−HA5	2.745	O4^{iv}	O3−H8	2.647	O4^{viii}
O4−H1	2.771	O3^{ii}	O5−HB5	2.805	O3^{v}	O3−H7	2.664	O1^{viii}
N1−H6	2.987	O1^{iii}	O6−HB6	2.805	O2^{vi}	N1−H5	3.009	O5^{ix}
			N1−HA1	3.275q	O3^{vii}	N1−H5	3.135	O1^{x}
			N1−HA2	3.011	O1^{vii}	N1−H6	2.999	O2^{xi}

[a] Symmetry transformations used to generate equivalent atoms: (i) $-x+1, -y+1, -z+2$; (ii) $-x, -y, -z+1$; (iii) $x-1, y, z$; (iv) $-x+1, -y+3, -z+2$; (v) $-x, -y+3, -z+2$; (vi) $x-1, y, z$; (vii) $x+1, y, z$; (viii) $-x+2, -y+1, -z$; (ix) $-x+1, -y+1, -z$; (x) $x-{}^1/_2, -y+{}^1/_2, z+{}^1/_2$; (xi) $-x+{}^3/_2, y-{}^1/_2, -z-{}^1/_2$.

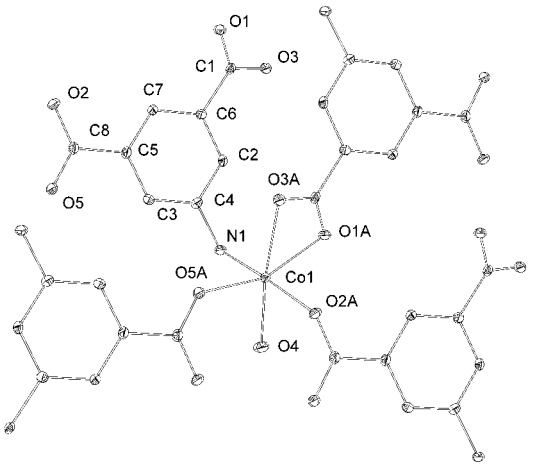

Figure 1. ORTEP representation of the symmetry-expanded local structure for **1** (30% probability ellipsoids).

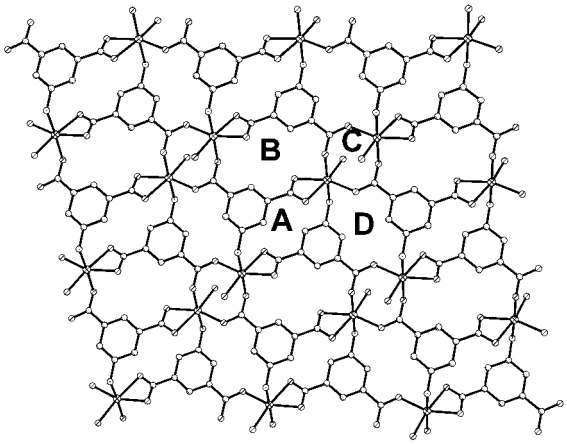

Figure 2. A view of **1** showing how the organization of the four different subrings (marked with **A**, **B**, **C**, and **D**) contributes to the construction of the infinite honeycomb sheet.

lamellar structure of **1**, showing the coordination mode for the AIP ligand, is shown in Figure 2. In polymer **1**, each AIP ligand employs its carboxylate groups and amino group in turn to coordinate to four metal centers. So the unique coordination modes for the ligand can be described as following: one of its two carboxylate groups bridges to two different Co^{II} cations (Co−O = 2.012(2) and 2.114(2) Å), and another one coordinates to a third Co^{II} center as bidentate (Co−O = 2.098(2) and 2.211(2) Å), while the amino group bonds to the fourth Co^{II} center (Co−N = 2.186(2) Å). Thus, the coordinated geometry around each Co^{II} cation is a distorted octahedron, comprising four oxygen atoms from three carboxylate groups, one amino nitrogen atom from the fourth ligand, and an aqua ligand (Co−O = 2.147(2) Å). The most interesting feature for polymer **1** is that the AIP ligands link cobalt centers in different ways to produce four different subrings **A**, **B**, **C**, and **D**, which are 12-membered, 14-membered, 8-membered, and 14-membered rings with Co···Co distances of 7.997, 7.656, 4.361, and 7.595 Å, respectively. In other words, the 2D network of **1** can also be envisioned as being built up from the interlocking motifs **[A + B + C + D]** through sharing cobalt atoms. Finally, the $\{CoAIP\}_n$ layers are assembled into a 3D network via interlameller hydrogen bonding involving the coordinated water molecules and amino groups with carboxylate groups (Figure 3).

The structure determination reveals that **2** is an infinite neutral linear polymer. The coordinated geometry around each Ni^{II} center is also a distorted six-coordinated octahedron. Different from the coordination mode in **1**, each AIP ligand employs its two carboxylate groups and one amino group in turn to coordinate to three metal centers. The unique coordination feature for the AIP ligand in **2** is that it uses one monodentate carboxylate group to bond to one Ni^{II} cation (Ni−O = 2.030(3) Å) and one bidentate carboxylate group to bond to another Ni(II) center (Ni−O = 2.046(4)-2.052(4) Å), while the amino group coordinates to the third Ni(II) center (Ni−N = 2.117(4) Å). Finally, two aqua ligands complete the octahedral environment for each nickel(II) atom (Figure 4). The two symmetry-related metal centers are linked by two AIP ligands to form a 12-membered macrocycle with Ni···Ni separation of 7.904 Å, which is further linked by another AIP ligand to an open railroad-like framework polymer (Figure 5). Most noticeable is that there also exist extended intermolecular hydrogen bonds among aqua ligands, the oxygen atoms of carboxylate groups, and amino groups, which connect each linear polymer into a three-dimensional framework (Figure 6).

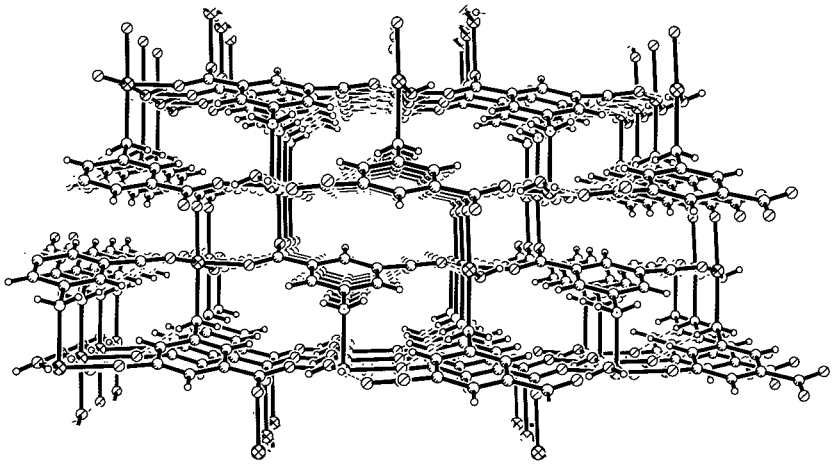

Figure 3. View of the molecular packing of **1**, down the *a* axis showing the interlameller linkage.

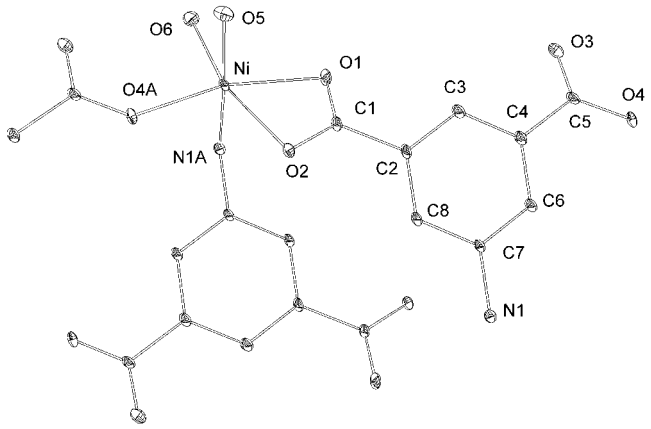

Figure 4. ORTEP representation of the symmetry-expanded local structure for **2** (30% probability ellipsoids).

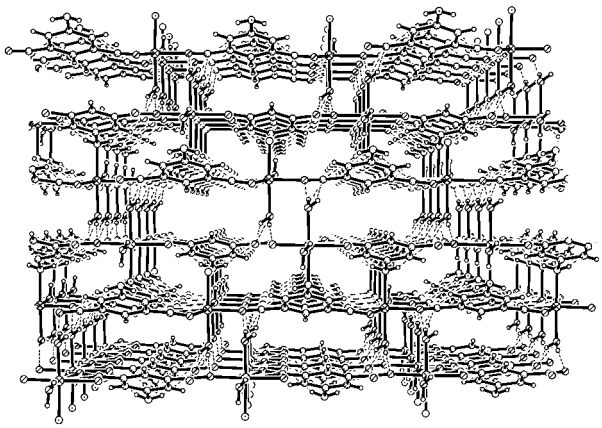

Figure 6. The packing of **2** viewed down the *a* axis, showing the connectivity of the railroad-like linear polymers via hydrogen bonding.

Single-crystal X-ray diffraction study reveals that polymer **3**, which crystallizes in the space group $P2(1)/n$, consists of infinite layers of alternating Zn(II) cations and AIP ligands. Different from **1** and **2**, each zinc ion is in a four-coordinated tetrahedron defined by two identical carboxylate groups (Zn−O = 1.954(3) and 1.974(3) Å), one amino group (Zn−N = 2.031(4) Å) of three different AIP ligands, and one water molecule ligand (Zn−O = 1.965(4) Å) (Figure 7). Also different from the coordination modes in **1** and **2**, each AIP ligand in **3** in turn employs its two monodentate carboxylate groups and one amino group to coordinate to three metal centers. Thus, three metal centers are linked by three ligands, into a 21-membered macrocycle, which is further linked to six nearest-neighbor Zn^{II} centers by three independent AIP ligands to give rise to a lattice plane with a cavity of 8.264 × 8.264 Å (Figure 8). It is very interesting to see that, in the same layer of **3**, all of the aqua ligands are oriented toward the same direction. Furthermore, all of these layers, where the aqua ligands are oriented in opposite directions, are linked together in pairs through strong hydrogen bonding into a three-dimensional framework. In short, the overall result of this arrangement for such a supramolecular lattice-like network is virtually based on covalent bonding and hydrogen-bonding interactions (Figure 9).

3.2. Magnetic Properties. The variation of the molar magnetic susceptibilities χ_M was investigated for compound **1** in the temperature range 5.2−299.3 K in a 10 kG applied field. Figure 10 shows the magnetic behavior of **1** in the forms of $\chi_M T$ vs T and χ_M^{-1} vs T plots. At 299.3 K, the $\chi_M T$ value is 2.193 emu K mol^{-1} per Co^{II}. Upon cooling to 5.2 K, the $\chi_M T$ values decrease gradually to 1.138 emu K mol^{-1}, indicating the presence of antiferromagnetic coupling in compound **1**. As shown in the χ_M^{-1} vs T plot, all data follow the Curie−Weiss law closely with $C = 2.264$ emu K mol^{-1}, and $\theta = -2.133$ K, corresponding to the parameter $g = 2.20$, which is comparable to that obtained by EPR measurement ($g = 2.2412$). The small θ value suggests that there is a weak antiferromagnetic interaction among cobalt(II) atoms transferred through AIP ligands. This result is consistent with its structure, where the closest cobalt(II) centers are separated by the carboxylate groups and AIP ligands in distances of 4.361 and 7.595 Å.

The temperature dependences of the magnetic susceptibilities were measured in the temperature range 299.4−5.0 K for compound **2**. Figure 11 shows the magnetic behavior of **2** in the form of $\chi_M T$ vs T and χ_M^{-1} vs T plots. At 299.4 K, $\chi_M T = 1.186$ emu K mol^{-1} per nickel(II). Upon cooling to 24.0 K, the $\chi_M T$ values increase continuously to a maximum 1.27 emu K mol^{-1}, indicating the presence of ferromagnetic coupling in **2**. Upon further cooling below 24.0 K, the $\chi_M T$ values decrease, to 0.991 emu K mol^{-1} at 5.0 K, which could be due to the zero-field splitting of the ground state. The χ_M^{-1} vs T is also almost linear in the whole temperature range. The data were therefore analyzed by the Curie−Weiss law, which led to the parameters $C = 1.1833$ emu K mol^{-1} and $\theta = 1.871$, corresponding to the parameter $g = 2.18$, which is also comparable to that obtained by EPR measurement ($g = 2.07$). The small θ value shows the weak ferromagnetic interactions in **2**. The paramagnetic behavior of **2** is also consistent with its structure, where the nickel(II) centers are separated by the AIP ligands in 7.904 Å.

4. Conclusion

In conclusion, three novel polymers with AIP ligands have been synthesized and characterized by magnetic measure-

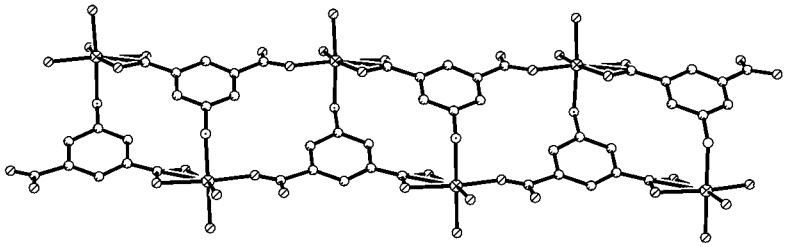

Figure 5. View of the extended structure of **2**, showing the railroad-like structure and the coordination mode for the AIP ligand.

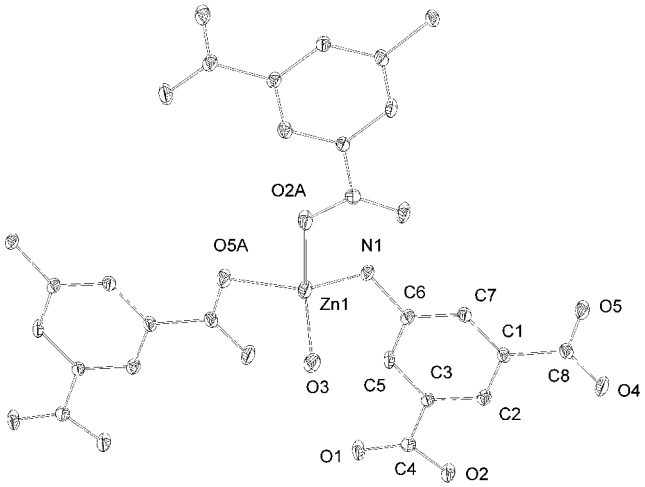

Figure 7. ORTEP representation of the symmetry-expanded local structure for **3** (30% probability ellipsoids).

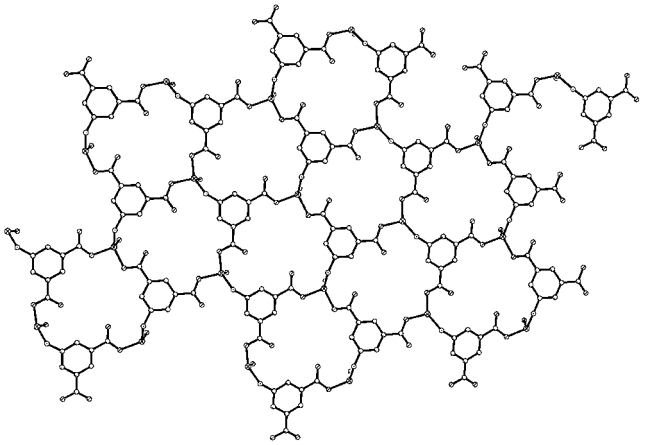

Figure 8. Side view of the grid lamellar framework of **3** and the coordination mode of the AIP ligand.

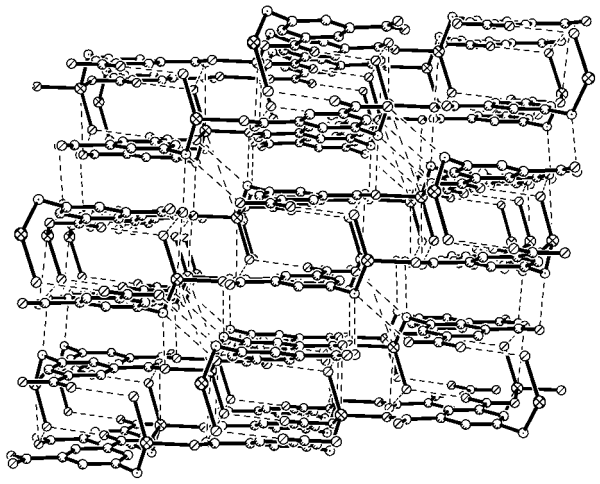

Figure 9. The molecular packing of **3** viewed down the *b* axis, showing the interlamellar connectivity via hydrogen bonding.

ments. Structural determinations of these three AIP-bridged transition metal complexes in this work have further shown that the ligand has the unique ability to form infinite lattices

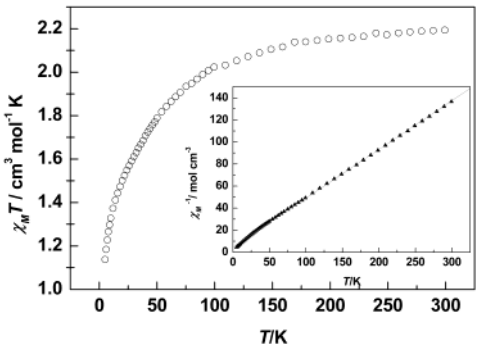

Figure 10. Plots of the experimental temperature dependences of $\chi_M T$ and χ_M^{-1} for **1**.

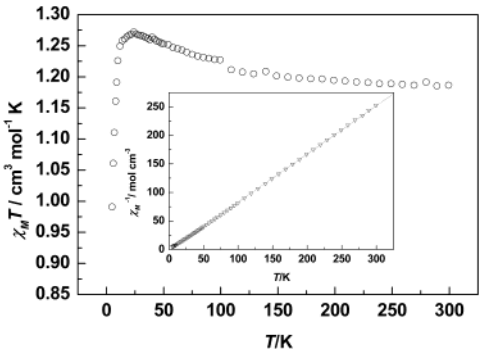

Figure 11. The $\chi_M T$ vs T and χ_M vs T plots for compound **2**.

with different transition metal ions and exhibited remarkable versatility in adopting different coordination modes. It is not yet fully understood what constitutes the major factor affecting the coordination modes in the given complexes; however, some conclusions can still be made: (1) Each transition metal ion has its own specific preference and different coordination geometries derived from the different ion radii and 3d electronic numbers, which can affect the interaction with carboxylate groups. (2) The reaction conditions, such as pH value, have important effects on the formation of products. The magnetic susceptibility measurements reveal that the antiferromagnetic coupling among the cobalt(II) cations in **1** and the ferromagnetic interactions occurring among the nickel(II) centers in **2** have been transferred through AIP ligands. On the basis of this work, further syntheses, structural diffraction studies, and the physical characterization of other transition metals as well as heterometal centers with the AIP ligand are also under way in our lab.

Acknowledgment. We gratefully thank the State Education Ministry, the National Natural Science Foundation of China (20073048), NSF of Fujian, and the Chinese Academy of Sciences for financial support.

Supporting Information Available: X-ray crystallographic files for $[Co(C_8NH_5O_4)(H_2O)]_n$ (**1**), $[Ni(C_8NH_5O_4)(H_2O)_2]_n$ (**2**), and $[Zn(C_8NH_5O_4)(H_2O)]_n$ (**3**) in CIF format. This material is available free of charge via the Internet at http://pubs.acs.org.

IC011182G